



## Subionospheric VLF observations of transmitter-induced precipitation of inner radiation belt electrons

U. S. Inan,<sup>1</sup> M. Golkowski,<sup>1</sup> M. K. Casey,<sup>1</sup> R. C. Moore,<sup>1</sup> W. Peter,<sup>1</sup> P. Kulkarni,<sup>1</sup> P. Kossey,<sup>2</sup> E. Kennedy,<sup>3</sup> S. Meth,<sup>4</sup> and P. Smit<sup>2</sup>

Received 17 October 2006; revised 24 November 2006; accepted 7 December 2006; published 23 January 2007.

[1] Ionospheric effects of energetic electron precipitation induced by controlled injection of VLF signals from a ground based transmitter are observed via subionospheric VLF remote sensing. The 21.4 kHz NPM transmitter in Lualualei, Hawaii is keyed ON-OFF in 30 minute periodic sequences. The same periodicity is observed in the amplitude and phase of the sub ionospheric propagating signals of the 24.8 kHz NLK (Jim Creek, Washington) and 25.2 kHz NLM (LaMoure, North Dakota) transmitters measured at Midway Island. Periodic perturbations of the NLK signal observed at Palmer, Antarctica suggest that energetic electrons scattered at longitudes of NPM continue to be precipitated into the atmosphere as they drift toward the South Atlantic Anomaly. Utilizing a model of the magnetospheric wave-particle interaction, ionospheric energy deposition, and subionospheric VLF propagation, the precipitated energy flux induced by the NPM transmitter is estimated to peak at  $L \sim 2$  and  $\sim 1.6 \times 10^{-4}$  ergs  $s^{-1} cm^{-2}$ . **Citation:** Inan, U. S., M. Golkowski, M. K. Casey, R. C. Moore, W. Peter, P. Kulkarni, P. Kossey, E. Kennedy, S. Meth, and P. Smit (2007), Subionospheric VLF observations of transmitter-induced precipitation of inner radiation belt electrons, *Geophys. Res. Lett.*, 34, L02106, doi:10.1029/2006GL028494.

### 1. Introduction

[2] The role of ground-based VLF transmitters in the precipitation of radiation belt electrons is a topic of growing interest. Previous evidence for transmitter-induced precipitation of electrons in the drift-loss-cone has been in the form of narrow resonant spectral peaks [Imhof *et al.*, 1974; Koons *et al.*, 1981] or coordinated wave-particle observations [Imhof *et al.*, 1981]. Direct observations of bursts of induced precipitation in the bounce loss cone were measured in the Stimulated Emission of Energetic Particles (SEEP) experiment carried out by Lockheed Palo Alto Research Laboratories and Stanford University [Imhof *et al.*, 1983; Inan *et al.*, 1985]. However, measurements of the ionospheric effects of transmitter precipitation have not been reported until now. Previous considerations of transmitter-induced precipitation [e.g., Inan *et al.*, 1984] have

concentrated on magnetosphericly 'ducted' propagation, placing the predicted precipitation regions in the vicinity of the major transmitters (e.g., NAA, NSS, and NLK), largely located at  $L$  shells of  $L > 2$ . At these higher  $L$  shells the energies of electrons experiencing gyro-resonance with the 20–25 kHz transmitter signals are only a few keV, outside the 100–300 keV energy range necessary for penetration of precipitating electrons into the nighttime D-region, so as to allow detection of the resultant ionospheric perturbations via subionospheric VLF methods. Other transmitters such as NWC and NPM were not even considered under this scenario of ducted wave-induced precipitation, since they are located at much lower  $L$ -shells, equatorward of the inner belt regions.

[3] Since it is now known that non-ducted VLF waves can efficiently precipitate detectable bursts of energetic electrons [Johnson *et al.*, 1999; Lauben *et al.*, 1999; Peter and Inan, 2004] the possibility of detection of precipitation induced by transmitters at lower  $L$ -shells has come to fore. Whistler-mode wave energy injected into the magnetospheric regions by such transmitters propagates in the non-ducted mode, permeating the inner belt and slot regions, where it can resonantly interact with electrons with higher resonant energies. Precipitating bursts of such energetic (>100 keV) electrons can thus create secondary ionization at altitudes below the nighttime VLF reflection height allowing detection via the subionospheric VLF method. The 464 kW NPM transmitter operating at 21.4 kHz and located on Lualualei, Hawaii ( $L = 1.17$ ) is one such transmitter that is well-positioned for this purpose and was thus selected for the controlled precipitation experiments the first results of which are reported herein.

### 2. Experimental Setup

[4] The NPM transmitter (20.4°N, 158.2°W) was modulated with a variety of ON/OFF keying formats (5-sec ON/5-sec OFF, 3-sec ON/2-sec OFF, etc) for 30 minutes every night beginning on August 25, 2005. Two-channel VLF receivers with 1.69 m<sup>2</sup> air-core loop antennas were installed on Midway Island (MI) and Waimea on Kauai Island (WM), while a similar receiver utilizing a 17.6 m<sup>2</sup> triangular antenna was installed at Kwajelein Atoll (KA). Figure 1 shows the geographic location of the NPM transmitter and the receivers as well as the area of predicted energetic electron precipitation determined using ray tracing and a test-particle model of the wave particle interaction [Bortnik *et al.*, 2006a; P. Kulkarni *et al.*, Precipitation signatures of ground-based VLF transmitters, submitted to *Geophysical Research Letters*, 2006, hereinafter referred to as Kulkarni *et al.*, submitted manuscript, 2006]. The receiver sites at MI

<sup>1</sup>Space, Telecommunications, and Radioscience Laboratory, Stanford University, Stanford, California, USA.

<sup>2</sup>Air Force Research Laboratory, Hanscom Air Force Base, Massachusetts, USA.

<sup>3</sup>Naval Research Laboratory, Washington, District of Columbia, USA.

<sup>4</sup>Defense Advanced Research Projects Agency, Arlington, Virginia, USA.

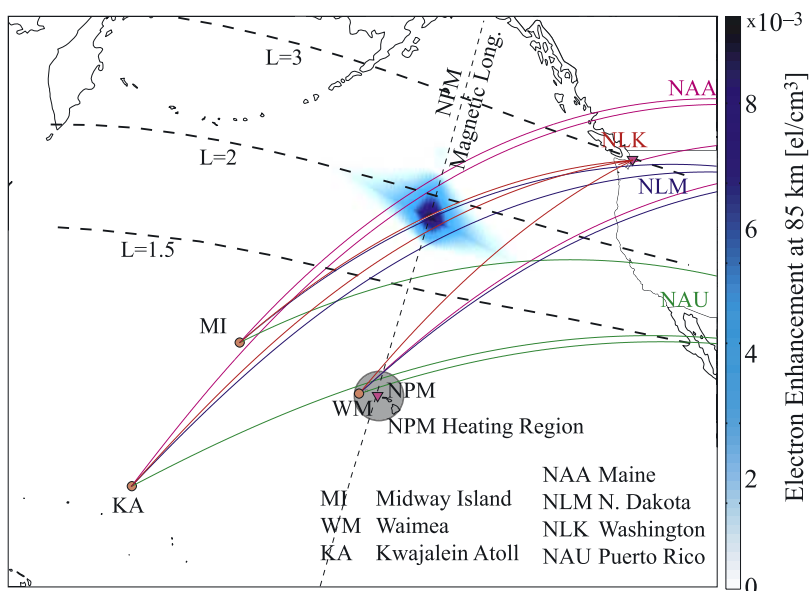


**Figure 1.** Map showing geographic and magnetic location of the NPM transmitter and great circle paths of the signals of the NAA, NLK, NLM, and NAU transmitters to receivers at Midway Island, Waimea, and Kwajalein Island. The electron density enhancement at 85 km resulting from the induced precipitation is superimposed on the map.

(28.21°N, 177.38W), KA (8.72°N, 167.72°E), and WM (21.96°N, 159.67°W) were chosen so as to receive the sub-ionospherically propagating signals of VLF transmitters located on the continental United States (NLK, NLM, NAA) which traverse the NPM induced precipitation region. Ionospheric perturbations caused by precipitating electrons are observed by detecting perturbations in the amplitude and phase of the traversing VLF signals in accordance with the well-documented subionospheric VLF method extensively used for detection of lightning-induced electron precipitation [Peter and Inan, 2004; Clilverd et al., 2002]. This VLF remote sensing technique is most sensitive to precipitating electrons in the 100–300 keV energy range, which deposit their energy (thus creating secondary ionization) near or immediately below the nighttime VLF reflection height of  $\sim 85$  km [Carpenter et al., 1997].

### 3. Observations

[5] Due to the inherently weak nature of the perturbation signature, Fourier and superposed epoch analyses were employed to detect NPM-keying periodicity in the signals of VLF transmitters passing under the precipitation region. Out of 357 thirty minute periods of keyed transmissions conducted between 25 Aug 2005 and 18 May 2006, evidence of ionospheric perturbation from electron precipitation was detected in 104 cases. Of 10 formats transmitted ranging from modulations of 8.3 mHz (1-min ON/1-min OFF) to 0.33 Hz (1-sec ON/2-sec OFF), precipitation was detected only for the 0.1 Hz (5-sec ON/5-sec OFF) and 0.2 Hz (3-sec ON/2-sec OFF) formats. All transmissions were conducted during local night time and approximately 67% of the 0.2 Hz formats and 35% of the 0.1 Hz formats exhibited evidence of precipitation. The greater prevalence of detections for the higher frequency format is believed to be partly due to the larger number of keying periods available for averaging within a half hour transmission

duration. The majority of detections were observations of perturbations on the NLK signal at MI, but several perturbations on the NLM-MI signal path were also observed. Figure 2 shows a typical case where the 24.8 kHz NLK and 21.4 kHz NLM signals observed at MI exhibit the 0.1 Hz keying frequency of the NPM transmitter (red trace in Figures 2a–2c). The effect is not observed during the preceding and following 30 minute periods (when NPM was not keyed, shown in the vertically displaced black traces in Figures 2a–2c) thus establishing the causative link between the NPM transmitter and the ionospheric perturbation. Figures 2d–2f show superposed epochs, illustrating the time-domain ionospheric perturbation signatures of amplitude change followed by recovery. These signal perturbations are similar but much smaller than typical lightning-induced events [Johnson et al., 1999; Peter and Inan, 2004]. While the NPM-keying periodicity was often clearly observed on several VLF signals paths to WM, the close proximity of this site to NPM compromised its usefulness in detection of precipitation since the dominating ionospheric effect observed was direct heating in line with Inan [1990] and Rodriguez et al. [1994]. Data from KA did not show any evidence of electron precipitation, possibly due to a combination of factors, as discussed below, although it is worth mentioning that data collection from this station was not as consistent, with only  $\sim 50\%$  of the keying periods covered.

[6] Observation of the NLK signal at Palmer Station, Antarctica (PA) allowed for detection of particles scattered into the drift loss cone, that precipitated at longitudes to the east of NPM. Using an IGRF model of the geomagnetic field, the bounce loss cone at NPM for  $L = 2$  is calculated to be only 17°, as compared to the drift loss cone of 23.5°, while the bounce loss cone along the great circle path from NLK to PA is 21°, thus much closer to the drift loss cone. As a result, particles experiencing NPM-induced pitch angle changes of only fractions of degrees are not observable at

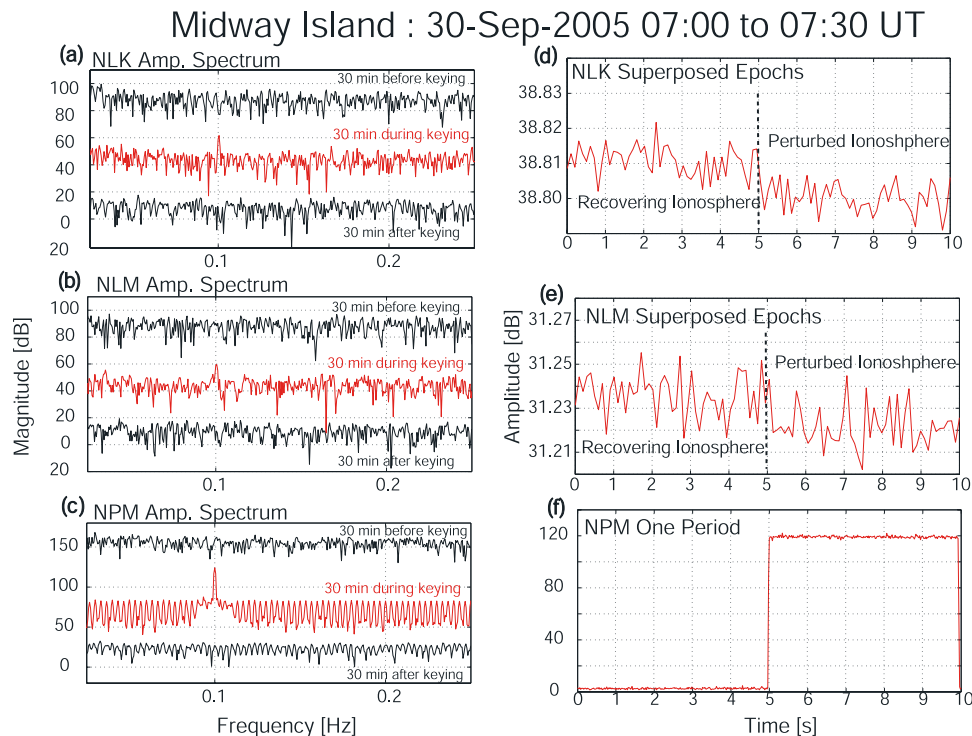


**Figure 2.** (a–c) Fourier frequency spectra for the 30-minute amplitudes of NPM, NLK and NLM measured at Midway Island (MI). Red trace in each panel is the spectrum during keying, black traces are spectra from 30 minutes before and after, displaced in vertical axis. NPM was modulated with a 5-sec ON/5-sec OFF format 0700–0730, the periodicity was also observed on NLK and NLM. (d–f) Super-posed epochs of data during keying with signatures exhibiting perturbed and recovering ionosphere characteristics.

the longitudes of the wave-particle interaction, but will precipitate into the lower ionosphere upon drifting eastward. Figure 3 shows 30 minute spectra of the NLK signal amplitude recorded at PA with a five minute time shift between each panel. On this day, NPM was keyed from 0945–1015 UT at 0.2 Hz. Although the thirty minute averages make it difficult to assign a specific time to each periodicity detection, the first appearance of the periodicity in Figure 3b (09:35–10:05), reaching maximum in Figure 3f (09:55–10:25) and decaying in Figure 3g (10:00–10:30) are in good agreement with the 13 minute drift time for 100 keV electrons between NPM and the NLK path to PA. It is important to note that the relationship between bounce and drift loss cone precipitation is more complicated than a simple displacement in time. Since the drift rates are functions of particle energy, a scattered burst of energetic electrons (with a range of energies) would disperse as it drifts eastwards, making direct comparisons of bounce and drift signatures on VLF paths difficult.

#### 4. Discussion

[7] The causative link between the NPM keying periodicity and its simultaneous observation on the NLM and NLK signal paths is interpreted to be due to the precipitation of energetic electrons based on solid agreement with theoretical predictions and the lack of any other means by which such modulation can occur. Cross-modulation of the signals inside the receiver is ruled out by the fact that the periodicity is not observed on transmitters other than NLK and

NLM. The  $>1000$  km distance between the NPM transmitter and the signal paths of NLM and NLK to MI makes it highly unlikely for any ionospheric heating effects. The drift loss cone precipitation observation on the NLK path to PA further rules out any such effect.

[8] On the other hand, observation of the perturbation effect predominantly on the NLK and sometimes on the NLM transmitter paths is consistent with expected magnetospheric electron precipitation. As is clear from Figure 1, these two transmitter paths traverse through the center of the induced-precipitation region. The NAA signal path skims the northern edge of this region, while the NAU path is too far south. The reason that observation on NLK was more common than on NLM is most likely due to the relatively higher signal-to-noise ratio (SNR) of NLK. The precipitation induced ionospheric perturbations are inherently small effects often overwhelmed by other perturbing sources including but not limited to local noise, lightning discharges and other nighttime ionospheric variations. Detecting such weak precipitation induced perturbations thus relies on the overall SNR of the received transmitter amplitude. Because of proximity and transmitting power, the SNR of NLK received at MI is 10 dB higher than that of NLM, which itself is 15 dB higher than that of NAA. The distant 100kW NAU transmitter signal is even weaker.

[9] The lower SNR for all these signals at KA is one of the likely reasons for the lack of detection of any precipitation effects at this site. Moreover, the overall electromagnetic noise environment at KA is much larger than MI, due to the presence of a military base and a relatively large

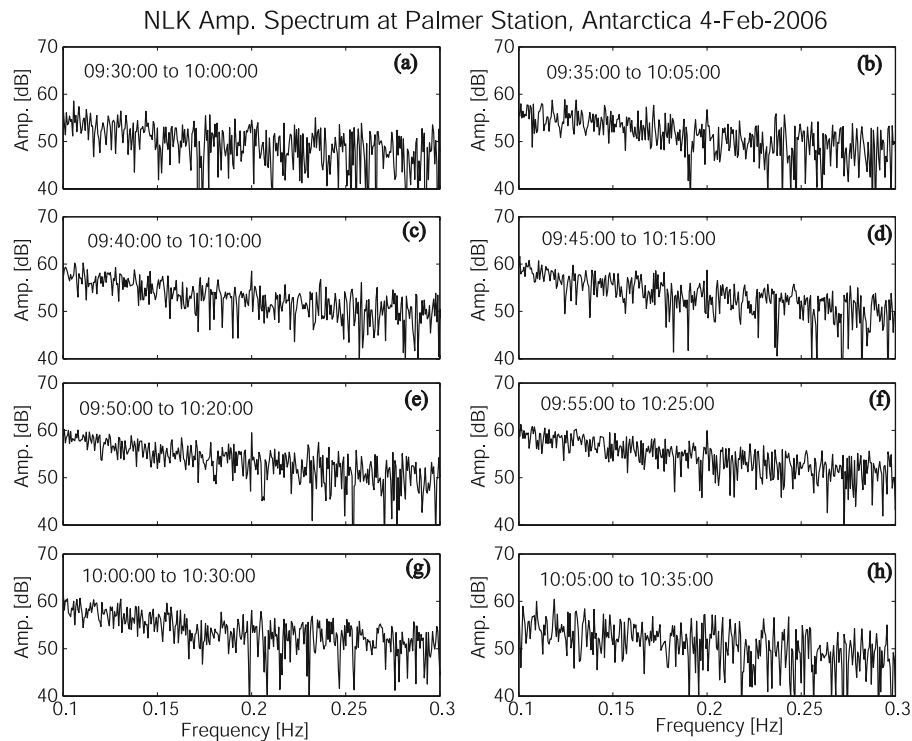


**Figure 3.** Spectrum of NLK transmitter amplitude observed at Palmer Station, Antarctica (PA) showing 0.2 Hz periodicity as evidence of drift loss cone precipitation induced by NPM keying 0945–1015 UT. (a–h) Each panel is a 30 minute spectrum of NLK displaced 5 minutes in time.

population, while MI is a bird sanctuary, with much less human activity. Thus, the SNR of the transmitter signals at KA are lower both due to the longer distances from the signal sources, and the greater background noise. It also should be mentioned that the detection of the effect at MI and not at KA, may also be contributed by the relative proximity of MI to the perturbed ionospheric region. In general, any ionospheric disturbance is likely to result in the excitation of a scattered VLF signal consisting of a range of VLF waveguide modes, some of which (especially higher order ones) would attenuate rapidly and not be visible at KA.

[10] During geomagnetically quiet times few energetic particles are present in the region between the edges of the bounce and drift loss cones. Since the difference between the drift loss cone ( $23.5^\circ$ ) and the bounce loss cone ( $17^\circ$ ) at the location of the NPM transmitter is relatively large, NPM-induced precipitation fluxes are generally expected to be larger and hence more readily detectable during injection events following disturbed periods. However, no clear correlation was found between days of observed precipitation and geomagnetic activity as manifested by the Kp and DST indices. Previous wave-particle interaction studies [Bortnik *et al.*, 2006b; Chang and Inan, 1983] all emphasize the key role of the particle distribution at the edge of the loss cone in determining the magnitude of precipitated electron flux. Thus the observed precipitation cases should be correlated with the near loss cone particle distribution at the local longitude of NPM. Unfortunately, the longitude of NPM in relation to the South Atlantic Anomaly necessitates a diminished near loss cone population under ambient conditions and local variations are often

lost in the cumulative averages represented by global indices. In this context, the NPM induced precipitation should be more consistently observed in the drift loss cone due to the higher concentrations of the near drift loss cone distribution. Drift loss cone precipitation was observed, but the energy dispersion in time and space involved with the drift process complicates detection since the NPM induced keying signature is often washed out and less defined.

## 5. Theoretical Analysis

[11] A comprehensive model consisting of three components: a model of wave-induced electron precipitation; a simulation of the energy deposition into the ionosphere resulting from precipitation flux; and a model of VLF sub-ionospheric signal propagation was used to quantify the observed precipitation signatures. Whistler wave propagation in the magnetosphere is simulated using the Stanford ray tracing code [Inan and Bell, 1977], including Landau damping effects according to the theoretical formulation of Brinca [1972]. The plasmaspheric cold plasma density is based on Carpenter and Anderson [1992], while the energetic trapped particle populations (with a square pitch angle distribution) are based on observations from the POLAR spacecraft [Bell *et al.*, 2002]. Pitch angle scattering of energetic particles into the loss cone by the whistler wave is calculated according to the work of Bortnik *et al.* [2006a], and yields precipitated flux as a function of energy, L-shell, longitude and time. The calculated precipitation flux is input into a Monte-Carlo simulation of the penetration of energetic electrons into the ionosphere to determine the energy deposition as a function of L-shell and altitude [Lehtinen

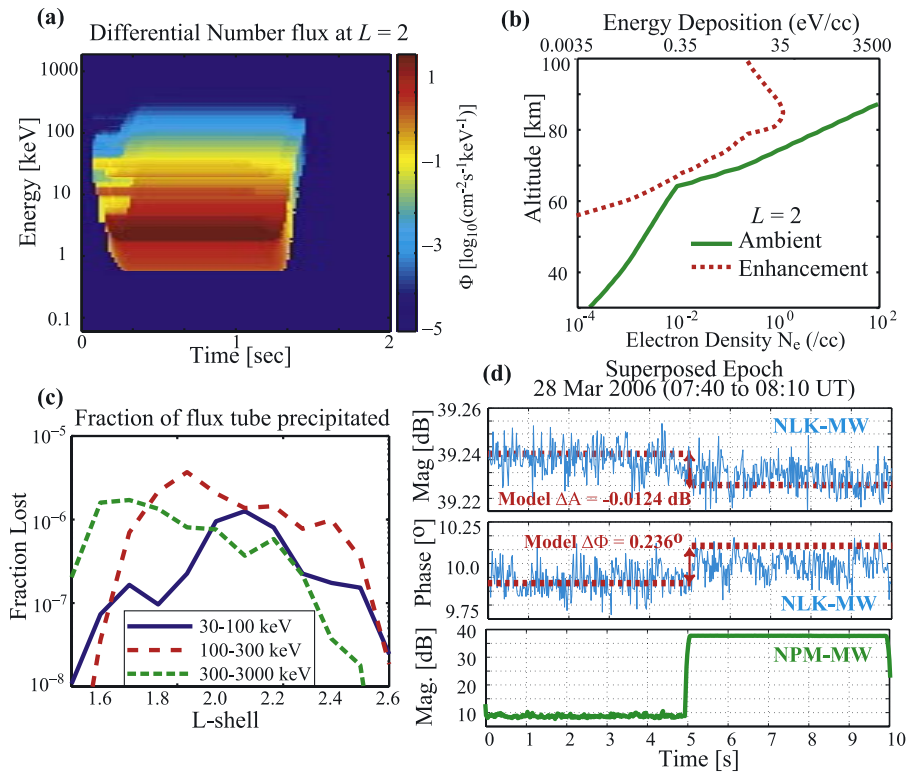


**Figure 4.** Comparison of VLF signal observations to model of wave-particle interaction, ionospheric energy deposition and VLF signal perturbation. (a) Modeled precipitated flux at  $L = 2$  for a 1 second NPM pulse. (b) Ionospheric ambient profile and density enhancement at  $L = 2$ . (c) Fraction of flux tube precipitated and (d) superposition of modelled and observed amplitude and phase changes for the NLK signal received at Midway.

*et al.*, 2001]. Assuming one ion-electron pair produced per 35 eV deposited [Rees, 1963], the disturbed ionospheric density profile is obtained. The disturbed ionospheric density is then input into a Finite Difference Frequency Domain (FDFD) model of subionospheric VLF signal propagation [Chevalier and Inan, 2007] to quantitatively relate the ionospheric density enhancements to the measured VLF signal perturbations.

[12] The precipitated flux predicted by the model is highly sensitive to the energy spectra, flux levels, and initial pitch angle distribution of the trapped electron population. Given the inherent uncertainty in these quantities, starting with an assumed trapped electron distribution will lead to expected differences between model and observations. However, since we seek to quantify the precipitation induced by NPM, the trapped flux levels were scaled down so that the subionospheric VLF amplitude perturbation predicted by the model matches the observations. The results of the model are summarized in Figure 4. Figure 4a shows the precipitated differential number flux at  $L = 2$  for a 1 second pulse of the NPM transmitter, with flux peaking at  $\sim 10 \text{ cm}^{-2}\text{s}^{-1}\text{keV}^{-1}$ . The ambient ionospheric electron density and the resulting density enhancement at  $L = 2$  is shown in Figure 4b. The peak enhancement occurs at  $\sim 85$  km altitude, the inferred nighttime reflection height for VLF signals [Carpenter *et al.*, 1997]. Figure 4d shows the amplitude and phase changes predicted by the model and observed for the NLK VLF signal recorded at Midway. The trapped energetic flux levels (see above) were scaled by a factor of 0.65 so that the model predicts a 0.008 dB and

0.15 degree changes in the NLK amplitude and phase, consistent with observations. The peak precipitation energy flux thus estimated by the model ( $E > 45$  keV) is  $1.6 \times 10^{-4} \text{ ergs s}^{-1} \text{ cm}^{-2}$  at  $L \sim 2$ . This flux level is about ten times less than that associated with lightning-induced electron precipitation (LEP) events [Voss *et al.*, 1998], which exhibit a correspondingly larger VLF signal perturbation signature [Peter and Inan, 2004], detectable without superposed epoch averaging. Figure 4c shows the fraction of trapped flux precipitated from a flux tube as a function of  $L$ -shell at the geomagnetic longitude of NPM, for three different energy ranges. For the range 100 keV–300 keV, the fractional loss peaks at  $L \sim 1.9$  and  $10^{-6}$ , again, about ten times less than that associated with LEP events [Voss *et al.*, 1998].

## 6. Summary

[13] We have reported clear evidence of modulated precipitation of energetic electrons induced by modulated transmissions by the NPM transmitter. The precipitated energy flux induced by the NPM transmitter is estimated to peak at  $L \sim 2$  and  $\sim 1.6 \times 10^{-4} \text{ ergs s}^{-1} \text{ cm}^{-2}$ . Although the precipitation flux induced by the NPM transmitter is found to be relatively small (compared, for example, to LEP events), it should be noted that precipitation induced by other VLF transmitters may well be substantially higher, as evidenced by recent observations on DEMETER spacecraft [Sauvaud *et al.*, 2006] and model calculations (Kulkarni *et al.*, submitted manuscript, 2006). The observation and

quantitative assessment of energetic electron precipitation induced by the NPM ground based transmitter is a key step in quantification of the loss of radiation belt electrons, including the contribution of current and potential man-made sources.

[14] **Acknowledgments.** This work was supported by the Defense Advanced Research Projects Agency (DARPA) and the High Frequency Active Auroral Research Program (HAARP) under ONR grants N00014-06-1-1036 and N00014-03-1-0630 to Stanford University. Special thanks to the NPM operators and U.S. Fish and Wildlife Service on Midway Island for the transmissions and data collection.

## References

- Bell, T. F., U. S. Inan, J. Bortnik, and J. D. Scudder (2002), The Landau damping of magnetospherically reflected whistlers within the plasma-sphere, *Geophys. Res. Lett.*, *29*(15), 1733, doi:10.1029/2002GL014752.
- Bortnik, J., U. S. Inan, and T. F. Bell (2006a), Temporal signatures of radiation belt electron precipitation induced by lightning-generated MR whistler waves: 1. Methodology, *J. Geophys. Res.*, *111*, A02204, doi:10.1029/2005JA011182.
- Bortnik, J., U. S. Inan, and T. F. Bell (2006b), Temporal signatures of radiation belt electron precipitation induced by lightning-generated MR whistler waves: 2. Global signatures, *J. Geophys. Res.*, *111*, A02205, doi:10.1029/2005JA011398.
- Brinca, A. (1972), On the stability of obliquely propagating whistlers, *J. Geophys. Res.*, *77*, 3495–3507.
- Carpenter, D. L., and R. R. Anderson (1992), An ISEE/whistler model of equatorial electron density in the magnetosphere, *J. Geophys. Res.*, *97*, 1097–1108.
- Carpenter, D. L., M. Galand, T. F. Bell, V. S. Sonwalkar, U. S. Inan, J. LaBelle, A. J. Smith, T. D. G. Clark, and T. J. Rosenberg (1997), Quasiperiodic 5–60 s fluctuations of VLF signals propagating in the Earth-ionosphere waveguide: A result of pulsating auroral particle precipitation?, *J. Geophys. Res.*, *102*(A1), 347–361.
- Chang, H. C., and U. S. Inan (1983), Quasi-relativistic electron precipitation due to interactions with coherent VLF waves in the magnetosphere, *J. Geophys. Res.*, *88*(A1), 318–328.
- Chevalier, M. W., and U. S. Inan (2007), A technique for efficiently modeling long path propagation for use in both FDFD and FDTD, *IEEE Antennas Wireless Propag. Lett.*, in press.
- Ciliverd, M. A., T. D. G. Clark, E. Clarke, H. Rishbeth, and T. Ulich (2002), The causes of long-term change in the aa index, *J. Geophys. Res.*, *107*(A12), 1441, doi:10.1029/2001JA000501.
- Imhof, W. L., E. E. Gaines, and J. B. Reagan (1974), Evidence for the resonance precipitation of energetic electrons from the slot region of the radiation belts, *J. Geophys. Res.*, *79*, 3141.
- Imhof, W. L., R. R. Anderson, J. B. Reagan, and E. E. Gaines (1981), The significance of VLF transmitters in the precipitation of inner belt electrons, *J. Geophys. Res.*, *86*, 11,225–11,234.
- Imhof, W. L., J. B. Reagan, H. D. Voss, E. E. Gaines, D. W. Datlowe, J. Mobilia, R. A. Helliwell, U. S. Inan, J. P. Katsufraakis, and R. G. Joiner (1983), The modulated precipitation of radiation belt electrons by controlled signals from VLF transmitters, *J. Geophys. Res.*, *10*, 615–618.
- Inan, U. S. (1990), VLF heating of the lower ionosphere, *J. Geophys. Res.*, *17*, 729–732.
- Inan, U. S., and T. F. Bell (1977), The plasmapause as a VLF wave guide, *J. Geophys. Res.*, *83*(19), 2819–2827.
- Inan, U. S., H. C. Chang, and R. A. Helliwell (1984), Electron precipitation zones around major ground-based VLF signal sources, *J. Geophys. Res.*, *89*(A5), 2891–2906.
- Inan, U. S., H. C. Chang, R. A. Helliwell, W. L. Imhof, J. B. Reagan, and M. Walt (1985), Precipitation of radiation belt electrons by man-made waves: A comparison between theory and measurement, *J. Geophys. Res.*, *90*(A1), 359–369.
- Johnson, M. P., U. S. Inan, S. J. Lev-Tov, and T. F. Bell (1999), Scattering pattern of lightning-induced ionospheric disturbances associated with early/fast VLF events, *Geophys. Res. Lett.*, *26*(15), 2363–2366.
- Koons, H. C., B. C. Edgar, and A. L. Vampola (1981), Precipitation of inner zone electrons by whistler mode waves from the VLF transmitters UMS and NWC, *J. Geophys. Res.*, *86*, 640–648.
- Lauben, D. S., U. S. Inan, and T. F. Bell (1999), Poleward-displaced electron precipitation from lightning-generated oblique whistlers, *Geophys. Res. Lett.*, *26*(16), 2633–2636.
- Lehtinen, N. G., U. S. Inan, and T. F. Bell (2001), Effects of thunderstorm-driven runaway electrons in the conjugate hemisphere: Purple sprites, ionization enhancements, and gamma rays, *J. Geophys. Res.*, *106*(A12), 28,841–28,856.
- Peter, W. B., and U. S. Inan (2004), On the occurrence and spatial extent of electron precipitation induced by oblique nonducted whistler waves, *J. Geophys. Res.*, *109*, A12215, doi:10.1029/2004JA010412.
- Rees, M. H. (1963), Auroral ionization and excitation by incident energetic electrons, *Planet. Space Sci.*, *11*, 1209–1218.
- Rodriguez, J. V., U. S. Inan, and T. F. Bell (1994), Heating of the nighttime D region by very low frequency transmitters, *J. Geophys. Res.*, *99*(A12), 23,329–23,338.
- Sauvaud, J. A., T. Moreau, R. Maggiolo, C. Jacquy, M. Parrot, and J.-A. Berthelier (2006), Interaction of inner belt electrons with human-made VLF waves: Inner belt energy structuring, *Geophys. Res. Abstr.*, *8*, 09727.
- Voss, H. D., M. Walt, W. L. Imhof, J. Mobilia, and U. S. Inan (1998), Satellite observations of lightning-induced electron precipitation, *J. Geophys. Res.*, *103*(A6), 11,725–11,744.
- M. K. Casey, M. Golkowski, U. S. Inan, P. Kulkarni, R. C. Moore, and W. Peter, STAR Laboratory, Stanford University, Stanford, CA 94305, USA. (mag41@stanford.edu)
- E. Kennedy, Naval Research Laboratory, Washington, DC 20375, USA.
- P. Kossey and P. Smit, Air Force Research Laboratory, 29 Randolph Rd., Hanscom Air Force Base, MA 01731-3010, USA.
- S. Meth, Defense Advanced Research Projects Agency, Arlington, VA 22203, USA.